ELSEVIER

Journal of Pharmaceutical and Biomedical Analysis
19 (1999) 15–32

JOURNAL OF
PHARMACEUTICAL
AND BIOMEDICAL
ANALYSIS

Chemical profiles and monitoring dynamics at an individual nerve cell in *Planorbis corneus* with electrochemical detection

Brian B. Anderson, Andrew G. Ewing *

Pennsylvania State University, Department of Chemistry, 152 Davey Laboratory, University Park, PA 16802, USA

Received 27 January 1998; received in revised form 3 April 1998; accepted 3 April 1998

Abstract

The identified dopamine cell of *Planorbis corneus* is described as a model system to study neurotransmitter storage and dynamics. Techniques developed with this model system include capillary electrophoresis with electrochemical detection and microelectrochemistry at single cells. These techniques provide a powerful combination to examine single cell neurochemistry. Whole cell and cytoplasmic dopamine concentrations have been quantified with capillary electrophoresis. Additionally, this technique has been used to profile amino acids and to quantify two compartments of neurotransmitter in a single cell. Individual exocytosis events have been monitored at the cell body of the dopamine cell of *P. corneus* with microelectrodes. In this case, two different types of vesicles have been identified based on the amount of transmitter released. The psychostimulant, amphetamine, has been shown to selectively affect the amount of dopamine in these vesicles with lower to higher doses affecting the larger to smaller vesicle types, respectively. Microelectrochemistry at single nerve cells has also been used to demonstrate reverse transport of dopamine across the cell membrane and to suggest a role of this process in the molecular mechanism of amphetamine.

Keywords: Single cell electrochemistry; Exocytosis; Reverse transport; Dopamine storage; Amino acid profiling; Amperometry; Voltammetry

1. Introduction

To understand the chemistry of the brain is a project of great importance. However, there are many difficulties in analyzing the brain chemistry. The nervous system is a myriad of cells and combinations of these cells form areas of the brain that control everything from emotions to muscle movement. There are complex biological pathways to be understood. Many chemicals that act as messengers and modulators are present at low quantities and are sequestered in small volumes. In addition, many cells, or groups of cells, interact with one another to yield a biological response.

* Corresponding author. Tel.: +1-814-863-4563; Fax: +1-814-863-8081; e-mail: age@psuvm.psu.edu.

0731-7085/99/$ - see front matter
PII S0731-7085(98)00088-0

Electrochemical methods provide the means to simplify many of the problems encountered in neurochemical analysis. Although there are many compounds of neurological interest, only a few demonstrate redox chemistry at potentials attainable for electrochemical research. This gives electrochemical methods a unique chemical selectivity so that a single or perhaps a few compounds can be measured in a mixture of many other compounds. To minimize tissue damage and to achieve spatial selectivity, electrochemical probes must be fabricated routinely with total tip sizes that are small relative to the size of the tissue sample being analyzed. The spatial selectivity provided by the small size of the probes and the chemical selectivity provided by electrochemistry makes it an ideal technique for measuring target compounds in specific brain regions.

Another way to simplify neurochemical analysis is to study single cells. Electrochemistry is ideal for single cell analysis since the probes are so small, selective, and sensitive. Electrochemistry has been used, alone and in combination with a micro-scale separation technique, to study chemical storage and dynamics in many cell types [1,2]. In particular, electrochemical analysis of an invertebrate single cell model of neurotransmission, the giant dopamine cell (GDC) of the pond snail, *Planorbis corneus*, has provided some key information for dopamine (DA) neurotransmission.

This manuscript reviews the many electrochemical experiments that have been performed on the GDC. Background on the GDC and the methodology used to analyze it will be outlined first followed by a description of several key experiments. The experiments reviewed represent advances in both neurochemical studies and micro-scale analytical chemistry. Capillary electrophoresis has been used with electrochemical detection (CE-EC) to profile the primary amine content of the GDC [3] and also to study DA storage [4]. Voltammetric microelectrodes have been used to measure DA release by exocytosis [5] and reverse transport [6] from the cell body of the GDC. In addition, the dose dependent effect of the psychostimulant amphetamine on multiple vesicular stores of DA has been studied using microelectrodes [7].

1.1. P. corneus

The brain of the pond snail *P. corneus* contains an easily identifiable cell known as the GDC. The GDC is a useful single cell model system for studying chemical profiles and dynamics in neurons for several reasons. It is a large cell, located in a constant position in the brain of the animal. It contains femtomoles of DA, an electroactive neurotransmitter, of which only 2% is cytoplasmic [8]. The other 98% of the DA is presumably stored in vesicles that are released by calcium ion-dependent exocytosis from the cell body [5]. Excess cytoplasmic DA is removed from the cell by a nomifensine-sensitive DA transporter operating in reverse (reverse transport) [6]. In addition, DA synthesis and metabolism follows the same pathway as in mammalian neurons [9].

To perform the experiments described in this review, individual snails are pinned to a wax coated dish and dissected to reveal the brain of the animal. Fig. 1 is a photomicrograph of the brain of *P. corneus* following the dissection,

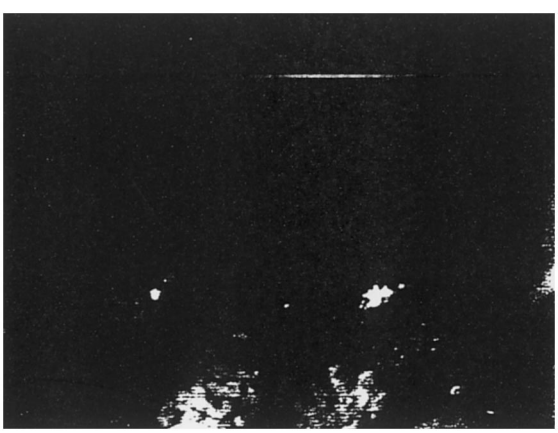

Fig. 1. Photomicrograph of the ventral side of the pedal ganglion of *P. corneus*. Typically, seven to ten pins are used to hold the ganglia ring against the dissection wax (not visible in the photomicrograph). The rightmost black arrow is pointing at the GDC, which can be seen beneath the transparent tissue surrounding the ganglion. The GDC is easily identifiable based on its large size and its location near the statocyst (leftmost arrow). The horizontal field of view of the photomicrograph is $\sim$1.6 mm. From Anderson et al. [10], with permission.

which is described elsewhere [10]. Many individual cells can be seen beneath the membranes that hold the cells in place. The GDC is the large cell (rightmost arrow) near the statocyst (leftmost arrow) of the left pedal ganglion. The membranes covering the cells are either partially or wholly removed to do various electrochemical experiments. Experiments are performed in the dish with the animal alive and functioning at the time of the experiment.

1.2. Microvoltammetric electrodes

Voltammetric microelectrodes have been used to study neurochemistry for many years [11–13]. Intracellular voltammetry has been used to measure drugs and neurotransmitters in single invertebrate neurons including identified neurons in *Aplysia californica* and the GDC [8,14,15]. And in 1990, microvoltammetric electrodes were first used to measure vesicular release of neurohormone (exocytosis) from single adrenal chromaffin cells in culture [16].

Although there are many materials and geometries used for electrode construction [17], the most common electrode is the disk electrode fabricated from a carbon fiber. To make a carbon fiber microelectrode [18], typically a 5 or 10 μm carbon fiber is sealed in a pulled glass capillary with epoxy. The excess carbon is cleaved with a scalpel at the glass/fiber interface and the fresh surface is beveled flat at a 45° angle with a slurry of fine diamond paste on a rotating wheel. These electrodes can measure zeptomole quantities [19] of electroactive neurotransmitter on the sub-millisecond time scale. They can also be used to measure sub-micromolar concentrations of biogenic amines using fast scan cyclic voltammetry [20]. Although microelectrodes can be used for direct single cell analysis, they can also be used as a detector for microcolumn separations [21]. In particular, they can be used for detection in capillary electrophoresis, as discussed in the next section. Detection electrodes for capillary electrophoresis are fabricated the same way as above except they have a cylindrical geometry for increased electroactive area.

1.3. Capillary electrophoresis with electrochemical detection

Capillary electrophoresis (CE) is a low volume sampling, high efficiency separation technique that separates molecules based on their differential size to charge ratio. Fig. 2(A) is a schematic of a CE experiment. A buffer filled fused silica capillary is suspended across two buffer reservoirs and a high potential field is applied across the capillary. One important aspect of CE is that the high potential field used as the separative force causes a bulk solvent flow termed electroosmotic flow (EOF). EOF allows cationic, anionic, and neutral molecules to be injected at one end of the separation capillary and detected at the other end. Typically, 10–30 kV is applied to the inlet reservoir and the detection reservoir is held at ground. Cations migrate toward the anode, in this format, from the injection end to the detection end of the capillary and separate based on differential electromigration. Neutral molecules elute as a single plug at a velocity indicative of the EOF. Anions migrate toward the cathode, or the injection end of the capillary, but they elute at the detection end because the EOF velocity is greater than their electrophoretic velocity.

One very important aspect of single cell analysis by CE is the detector. For red blood cells and lymphocytes, the detector must be able to detect as little as 200 zmol of material from a volume of 50–100 fl [22]. Laser induced fluorescence [23–27], mass spectrometry [28], immunoassay [29], and electrochemical detection [4,8,21,30–33] have been proven to be very useful in single cell analysis by CE. Since the GDC contains the electroactive neurotransmitter DA, electrochemistry is an ideal detection technique to use. Fig. 2(B) shows an electrochemical detector operating in the optimized end column mode [21]. For this detection format, the detection end of the capillary is etched with concentrated hydrofluoric acid (HF) to a cone so that the electrode can be easily manipulated into the end of the capillary with the aid of a microscope and micromanipulator. A reference electrode is also placed in the detection buffer reservoir to allow potentiostatic control of the electrochemical cell. As electroactive compounds

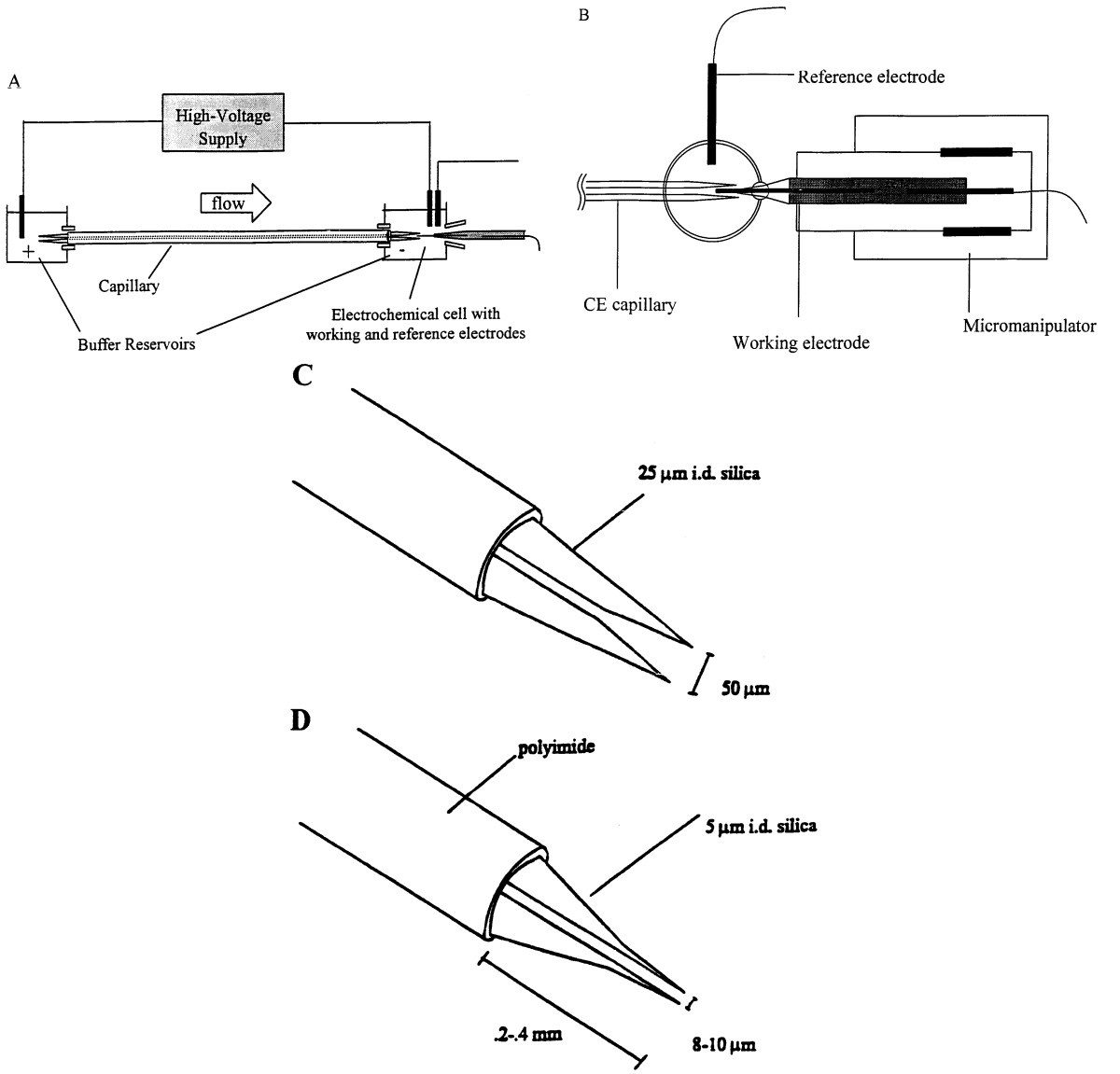

Fig. 2. Capillary electrophoresis with electrochemical detection and single cell injection protocols: (A) Schematic of capillary electrophoresis; (B) Schematic of optimized end column detection for capillary electrophoresis; (C) Injector for acquiring and injecting whole cells, constructed at the high voltage end of a 25-μm i.d. capillary; and (D) Injector for acquiring and injecting cytoplasmic smples at the high voltage end of a 5-μm i.d. capillary. From Swanek [90] with permission.

elute from the capillary, they are detected as faradaic current using either amperometry (constant potential) or scanning electrochemical detection. Amperometry, which provides extremely low detection limits [34], is used for high sensitivity work while scanning electrochemical detection [35] is used to identify the eluting components.

Equally important to single cell analysis is the ultralow volume sampling that CE affords. Fig. 2(C,D) is a schematic of two different types of single cell injections possible with CE. Fig. 2(C)

shows the protocol used for whole cell injections. The injection tip has been etched to a cone (similar to the exit end in optimized end column detection), and with the help of a microscope and micromanipulator, the capillary is manipulated so that it just touches the cell of interest. Once in place, a potential of ~ 10 kV is applied to the dish containing the cell and electroosmosis pulls the cell into the capillary. A plug of separation buffer is then pulled over the cell to initiate cell lysis. After the desired amount of time, the separation potential is applied and the contents of the cell are separated. The lyse time of the cell depends on the experiment and it can take up to 15 min in order for derivatization reactions to take place. In Fig. 2(D), the tip of the injection end of the capillary has been chemically etched with concentrated HF to a fine point that can be placed inside a large cell like the GDC to remove a small volume (pl-fl) of the cytoplasm by electrokinetic injection.

The combination of electrochemical detection and ultra small-volume sampling makes CE-EC an ideal technique for analysis of the GDC. Its usefulness has been proven in the experiments outlined below.

2. Chemical profiling by capillary electrophoresis with electrochemical detection

Early characterization experiments of the GDC used histochemical methods to determine DA in the GDC [36,37]. This powerful method gave researchers an idea of the total cellular DA, but did not indicate where in the cell all of the DA was contained. Capillary electrophoresis with electrochemical detection has allowed the dopamine concentration in the cytoplasm to be measured [32], the DA storage mechanism in the GDC to be investigated [4], and the primary amine content of the GDC to be determined [3].

2.1. Cytoplasmic dopamine concentration

To measure the cytosolic DA concentration, the injection technique shown in Fig. 2(D) was used to make single injections of as little as 50 pl of cytoplasm from five individual GDCs. For a 200 μm diameter, spherical cell, $\sim 1\%$ of the cytoplasm was removed with an injection of this magnitude. It was found that DA was present in the cytoplasm at 2.2 ± 0.52 μM and that dihydroxyphenylacetic acid (DOPAC), a metabolite of DA, was present at 5.4 ± 1.2 μM. The value for DA was in agreement with data obtained by intracellular voltammetry which suggested that DA was present at or below the detection limit of the sensor of 1.9 ± 0.3 μM [8]. These experiments provided evidence that most of the cellular DA was not accessible to the cytosol. Further information concerning DA storage in the GDC was provided by differential lysing experiments as described below.

2.2. Investigation of somatic dopamine storage

Neuronal DA is thought to be stored in two compartments: a functional compartment and a non-functional compartment [38,39]. The functional compartment contains newly synthesized and uptaken DA that is ready for release. The nonfunctional compartment contains long term stores of dopamine and is thought to be used in long term potentiation. CE-EC has been used to study this hypothesis using the GDC as a model system [4]. For this experiment, a whole GDC is injected in the capillary as shown in Fig. 2(C). The capillary is then transferred to the buffer reservoir containing the separation buffer, a short plug of this non-physiological buffer is pulled over the cell, and the potential is turned off for 1 min. During this time, the cell begins to lyse and the easily releasable, first compartment of DA is released as a plug into the capillary. When the separation potential is turned on again, the easily released DA migrates toward the detector while the DA in the non-functional compartment is still contained within the cell at the entrance of the capillary. Once the cell completely lyses, the nonfunctional DA is free to migrate toward the detector. The resulting electopherogram is shown in Fig. 3. Fig. 3(A) is a standard injection of DA, catechol (a neutral molecule), DOPAC, and uric acid. Fig. 3(B) shows two cationic peaks, a neutral peak and an anionic peak. The most interest-

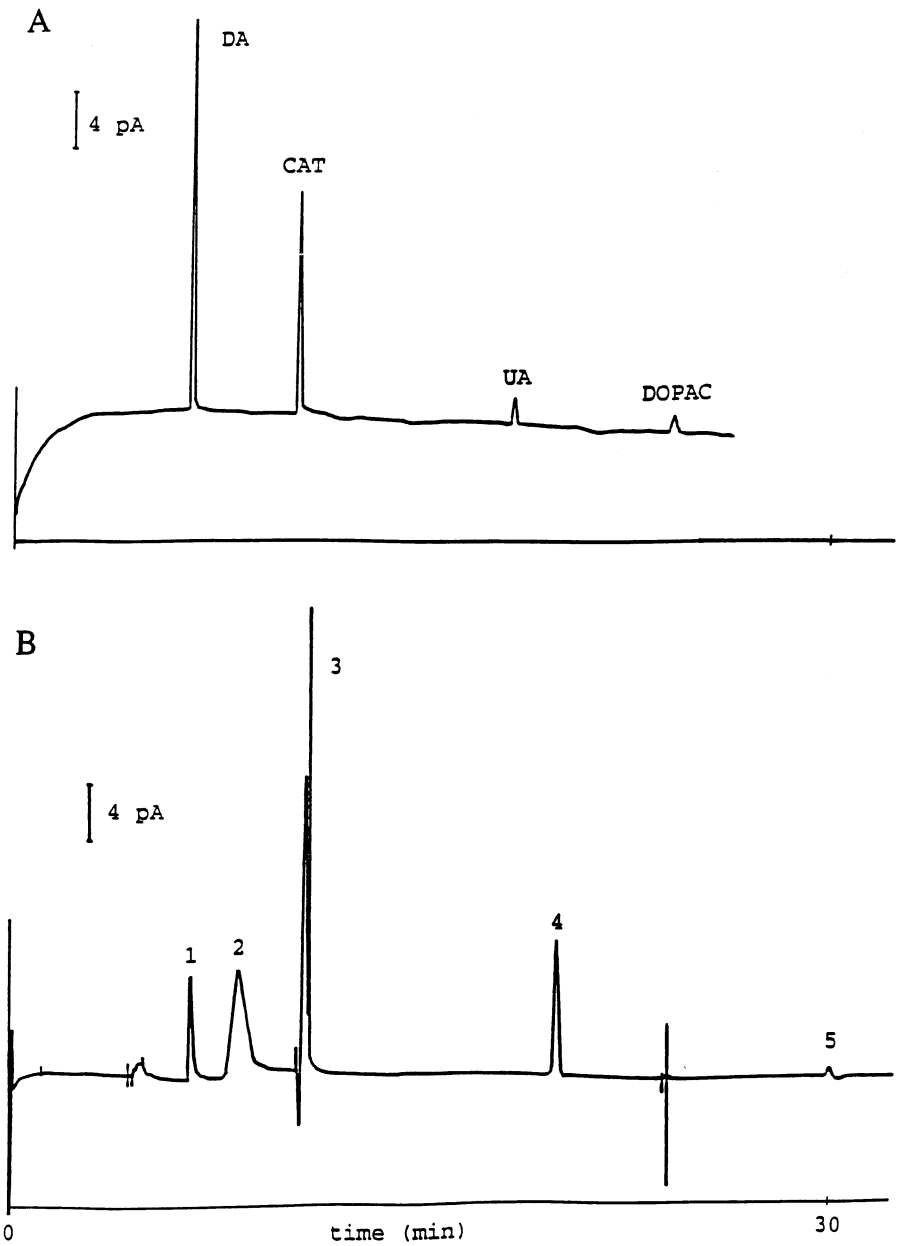

Fig. 3. Separation of two compartments of dopamine: (A) Capillary electrophoresis separation of a standard solution containing 10^{-6} M DA, Catechol (CAT), uric acid (UA), and DOPAC; injection volume was 3 nl based on EOF; separation capillary: 75-cm long, 25-μm i.d.; buffer: 25 mM MES at pH 5.65; separation potential, 25 kV; (B) Separation of components from an injected GDC after lysing in the capillary tip for 60 s with buffer. Separation conditions the same as for (A). From Kristensen et al. [4], with permission.

ing feature of Fig. 3(B) is the appearance of two cations. It is apparent that the first peak in Fig. 3(B) elutes at the same time as DA in the standard run. There is considerable evidence that the second cation is also DA and that together, these two cations represent the two storage compart-

ments of DA. First of all, it is known that the injected cell is the GDC based on its location in the brain of the snail. The electrophoretic mobility of the first peak matches that of DA in the standard injection, and if the wait time is increased to 5 min, only a single peak is observed due to complete cell lysis prior to the start of the separation. Also, by incubating the GDC for 60 min in 10 μM reserpine (a vesicle depleting agent), the amount of DA in the second peak is significantly decreased. All of these data suggest that DA is indeed stored in two compartments in the GDC and that CE-EC can be used to investigate this storage phenomenon. However, further evidence for the identification of the second cation in Fig. 3(B) is required.

Scanning electrochemical detection is well documented in separations [35,40–44]. Importantly, it has been demonstrated for CE [35,44]. For scanning electrochemical detection, the potential of the electrode shown in Fig. 2(B) is scanned over a range that will give the desired reaction for the species of interest. Different species can result in different current-potential traces thereby facilitating analyte identification. To identify the second cation in Fig. 3(B), the two compartment model experimental protocol described above has been used with scanning electrochemical detection [44].

Fig. 4(A) is a standard electropherogram with scanning electrochemical detection of DA and catechol. This 3D plot shows a complete voltammogram for each point in the electropherogram with the gray scale indicating current intensity. Fig. 4(B) is a plot similar to Fig. 4(A) except it is from an injection of a single GDC after a 1 min lyse time. Again, two cations are apparent. This plot, unlike the data in Fig. 3, contains voltammetric data as well as an electrophoresis axis. It is apparent from Fig. 4(B) that the voltammograms of both cations are nearly identical in shape. The similarity of the shape of the voltammetry is more clear in Fig. 4(C), which shows background subtracted voltammograms obtained from peaks 1 and 2 in Fig. 4(B). It is clear from the overlay that the two voltammograms are almost identical. Although the voltammogram for DA is not unique, there are no other compounds known in the left pedal ganglion of the brain of *P. corneus* that would match the voltammetry shown in Fig. 4(C). Therefore, this data strongly suggests that both peaks represent DA from the cell. The two peaks appear to represent two different compartments of DA in this cell.

Taken together, the differential lysing data, the reserpine pharmacology, and the scanning electrochemical detection, provide strong evidence that the GDC stores DA in a way consistent with the two compartment model. Other experiments including pharmacological manipulation of DA synthesis or inhibition of release of the first compartment should be possible and are currently under investigation.

Thus far, CE-EC has been shown to be very useful for the separation and quantification of an easily oxidizable species such as DA. The selectivity of electrochemical detection allows the determination of relatively few analytes at low levels present in a mixture of others that may be present at high levels. This selectivity can also be viewed as a drawback in that only those compounds that are easily oxidized are readily analyzed by electrochemistry. However, some classes of compounds that are not natively electrochemically active can be made so by derivatization.

2.3. Amino acid profiling

Napthelene-2,3-dicarboxaldehyde (NDA) reacts with primary amines in the presence of cyanide to form a cyano[*f*]benzoisoindole (CBI) derivative which is both fluorescent and electroactive [45–47]. Derivatization by NDA has been used to detect amino acids in single cells, tissue preparations, and microdialysis by exploiting the electroactive or fluorescent properties of the derivatized product [3,48–55]. Oates and Jorgensen and Oates et al. were the first to use the NDA derivatization reaction to profile amino acids in an invertebrate, the snail *Helix aspersia*, using microbore liquid chromatography with electrochemical detection [50,51]. Their work and that of Kennedy et al. [48], paved the way for amino acid profiling of the GDC by CE-EC.

The early single cell derivatization experiments have been performed in nl volume vials [48,49]. Single cells are isolated in the vial and then lysed.

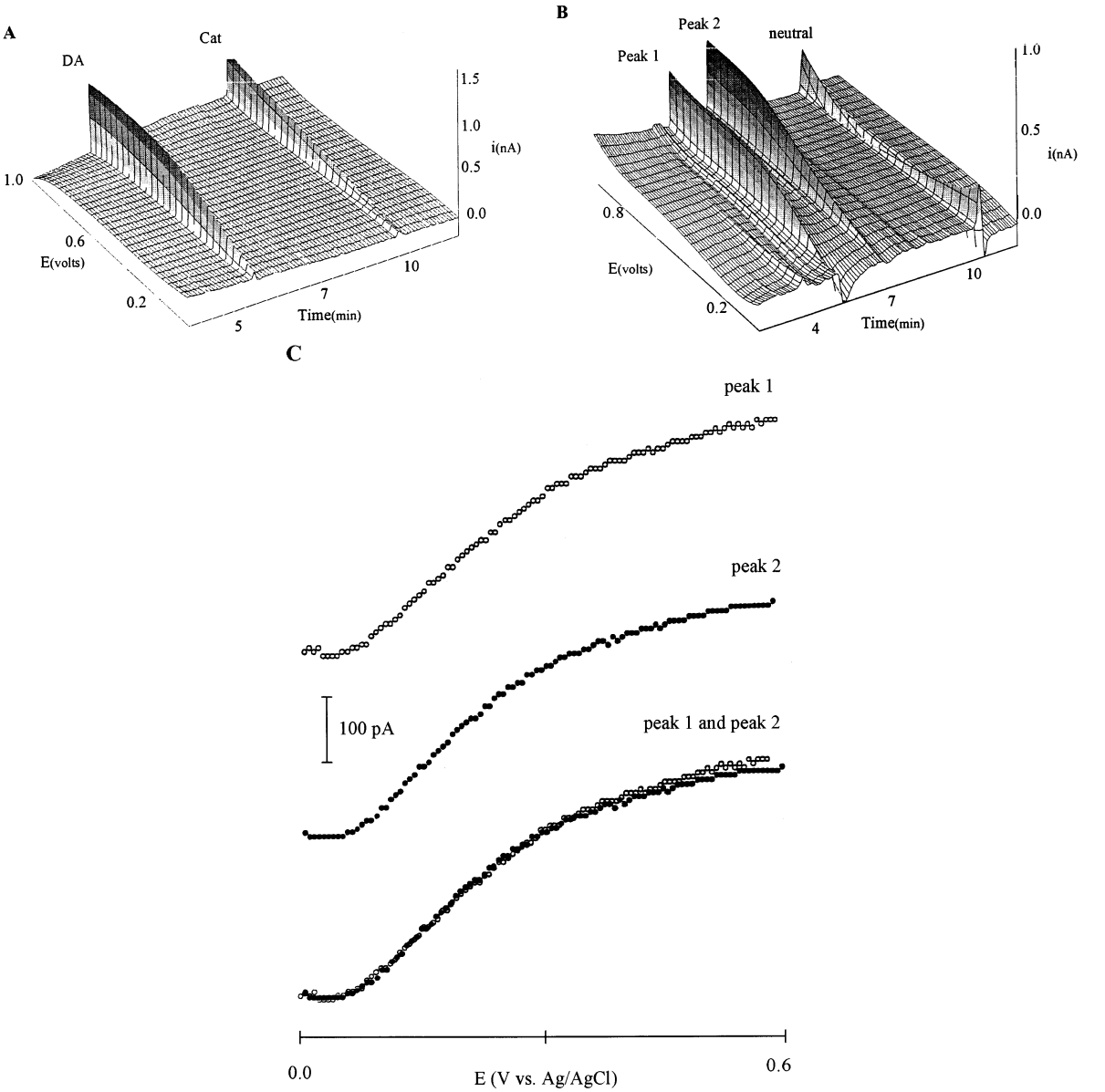

Fig. 4. (A) Three-dimensional electropherogram of the separtion of dopamine and catechol. Electrode potential is scanned from 0.0 to 1.2 V at a rate of 1 V s^{-1}; (B) Three-dimensional electropherogram of the electrophoretic separation of the contents of a single GDC; (C) Background-subtracted voltammograms obtained from peaks 1 and 2 in Fig. 4(B) and their overlay. Shown is the voltammogram from 0.0 to 0.6 V vs. Ag/AgCl. From Swanek et al. [44], with permission.

The contents of the cell are then derivatized in the vial and a fraction of the solution is injected into the capillary. Using the vials for reagent mixing increases dilution of the cellular contents and makes it necessary to use two internal standards for quantification. For amino acid profiling of the GDC, Swanek et al. [3] have used the on column single cell derivatization procedure reported by Gilman and Ewing [52]. For these experiments, a single GDC is injected into the etched capillary

entrance (Fig. 2(C)), the cell is lysed, and the contents are derivatized by electrophoretically introduced reagents. The derivatized primary amines are then separated and detected by CE-EC. By performing cell lysis and analyte derivatization in the entrance of the capillary, dilution effects are minimized and the need for internal standards is eliminated.

Fig. 5(A) shows the electrophoretic separation of NDA derivatized primary amines present in a single GDC. Identification of the peaks in Fig. 5(A) is made by comparing the electrophoretic mobility of each peak to that of a standard injection of primary amines shown in Fig. 5(B). Although peak 3 shows considerable tailing and, hence, peak broadening in Fig. 5(A), the mobility of this peak matches that of DA. NDA-derivatized DA appears to adsorb to the capillary leading to tailing in both the standard and cell experimental runs. Peak 4 matches the mobility of glycine in Fig. 5(B). Although peaks 5,6 and 7 do not match up exactly, they are expected to be DOPA (the metabolic precursor to DA), glutamic acid, and aspartic acid, respectively. The fact that peaks 5, 6, and 7 do not match exactly is likely do to the slowing of EOF seen in other single cell injections [32]. Quantification of primary amines in the GDC is shown in Table 1. It is notable that not all species are detected in each cell. The data in Fig. 5(A) represent cell 2 in Table 1. The values are much smaller than seen in other invertebrates [48].

Although CE-EC is very useful for measuring amounts of electrochemically active molecules in the GDC, it is inherently a static technique. Rapidly changing cellular events, such as exocytosis, are not recognized by CE-EC. Other electrochemical techniques, voltammetry and amperometry, can be used to directly measure rapid changes in concentration of electroactive neurotransmitters.

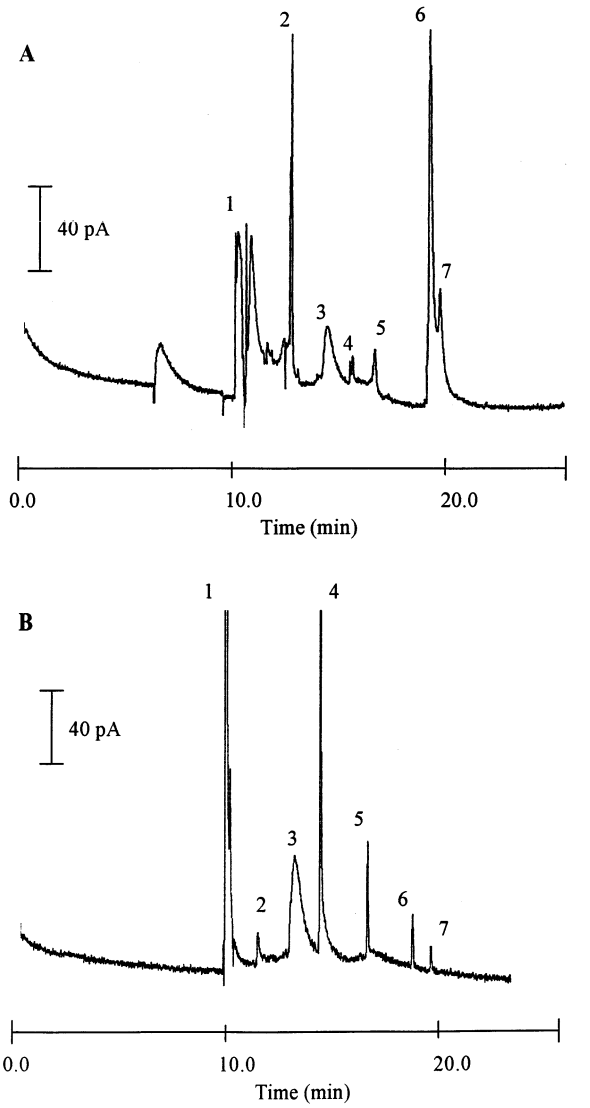

Fig. 5. (A) Electropherogram of a single dopamine neuron of *P. corneus* (cell no. 2, Table 2) detected electrochemically after on-column derivatization with NDA; (B) Electropherogram of 1.0×10^{-5} M amino acids run immediately before the cellular injection. Conditions: capillary, 25-μm i.d.; 85 cm length; injection, 10 s at 10 kV to pull cell into capillary, 15 s at 10 kV to pull derivatizing/lysing reagent over cell, 15 min to allow cell to lyse and content to react; standard injection, 5 s at 5 kV; separation potential, 25 kV; separation buffer, 10 mM borate, pH 9.0. Peaks have been identified as: 1, Arginine; 2, unknown; 3, Dopamine; 4, Glycine. Peaks 5, 6,and 7 are suspected to be DOPA, Glutamic acid, and Aspartic acid, respectively, that have been slowed owing to a change in electroosmotic flow during the cell separation. From Swanek et al. [3], with permission.

3. In vivo microelectrochemical characterization of the GDC

Electrochemical measurements of neurotransmitter concentration changes at single cells be-

Table 1
Quantitation[b] of amino acid content from giant dopamine cells removed from four *P. corneus* by capillary electrophoresis with amperometric detection[a]

	Cell 1	Cell 2	Cell 3	Cell 4
Arg[c]	–	–	–	–
DA	1.71	2.17	1.49	nd[e]
Gly	2.84	.386	1.32	nd[e]
Dopa[f]	4.62	2.64	7.07	14.7
Glu[f]	9.36[d]	26.5	13.8	18.0
Asp[f]	nd[d]	19.4	7.43	10.6

[a] From Swanek et al. [3], with permission.
[b] Amounts are presented in femtomoles (fmol).
[c] Arginine could not be quantitated due to interference from other neutral species.
[d] In cell 1 glutamic acid and aspartic acid were not resolved so the amount detected could be a contribution from both species.
[e] The electropherogram for cell 4 had a large neutral peak that obscured the peaks for DA and Gly.
[f] Identification of dopa, Glu, and Asp is highly tentative as it is based upon assumed 10% slowing of electroosmotic flow in cellular separation (see text for details).

came a reality in the early 1990s [16]. The authors used beveled carbon fiber microelectrodes [56] in both the voltammetric and amperometric mode to measure single exocytosis events from individual cells in culture [57]. The use of the ultra-small carbon fiber electrodes subsequently has been exploited by other scientists studying release of electroactive substances from various neurons and hormonal cells [1,2]. Microelectrochemistry has been used to measure DA release form the cell body of the GDC [5]. It is important that the GDC is the only model, to date, where release is measured from a single cell contained in a living animal. Initial studies suggested the existence of multiple classes of vesicles, a hypothesis subsequently studied by amphetamine pharmacology [7,58]. In addition, DA release from the cell body of the GDC by reverse transport has been measured using voltammetric microelectrodes and has been used to study the intracellular mechanism of action of amphetamine [6].

3.1. Electrochemical measurements of vesicular release from the cell body

Although neurotransmission is classically thought to happen at the synapse, there is a growing hypothesis that neurotransmitters are also released from elsewhere in neurons [59–66]. In fact, vesicular release has been shown to occur from the cell body of the GDC [5]. Fig. 6(A) shows the experimental setup for measuring DA release, by exocytosis, from the cell body of the GDC. For this experiment, the brain of *P. corneus* is exposed and the membranes covering the cells in the ganglion are partially removed. A microelectrode is micromanipulated up to the cell body with the aid of a microscope. A pulled glass capillary containing a stimulant, typically elevated potassium ion, is also micromanipulated to within 10–15 μm from the cell body. If the electrode is held at a constant potential when the cell is stimulated by pressure ejection of a chemical stimulant, all DA released under the electrode by calcium dependent exocytosis is immediately oxidized. The oxidation produces a current-time trace as shown in Fig. 6(B). Each vesicular packet of DA that is released (exocytosis event) results in a current transient characterized by a fast (<4 ms) rise time and an average base width of 14 ms. An expansion of the time axis is shown in Fig. 7(C). Each of the current transients represents a single vesicle fusing with the cell membrane and releasing its contents into the space between the cell and the electrode. It has been confirmed by intracellular sodium injection that release is from the GDC, not from other nearby neurons or glial cells. The identity of the released substance has been confirmed to be DA by voltammetry and capillary electrophoretic sampling and separation of the released substance [5].

One particularly interesting aspect of the data in Fig. 6 is that for most cells (24 out of 29), release occurs in bursts as shown in Fig. 6(D). The reason for this bursting pattern is presently unclear. One explanation is that the bursting occurs because of input from other cells. Others have shown pacemaker-like action potentials or membrane potential oscillations occur in molluscan and mammalian cells [67–72]. This hypothesis is

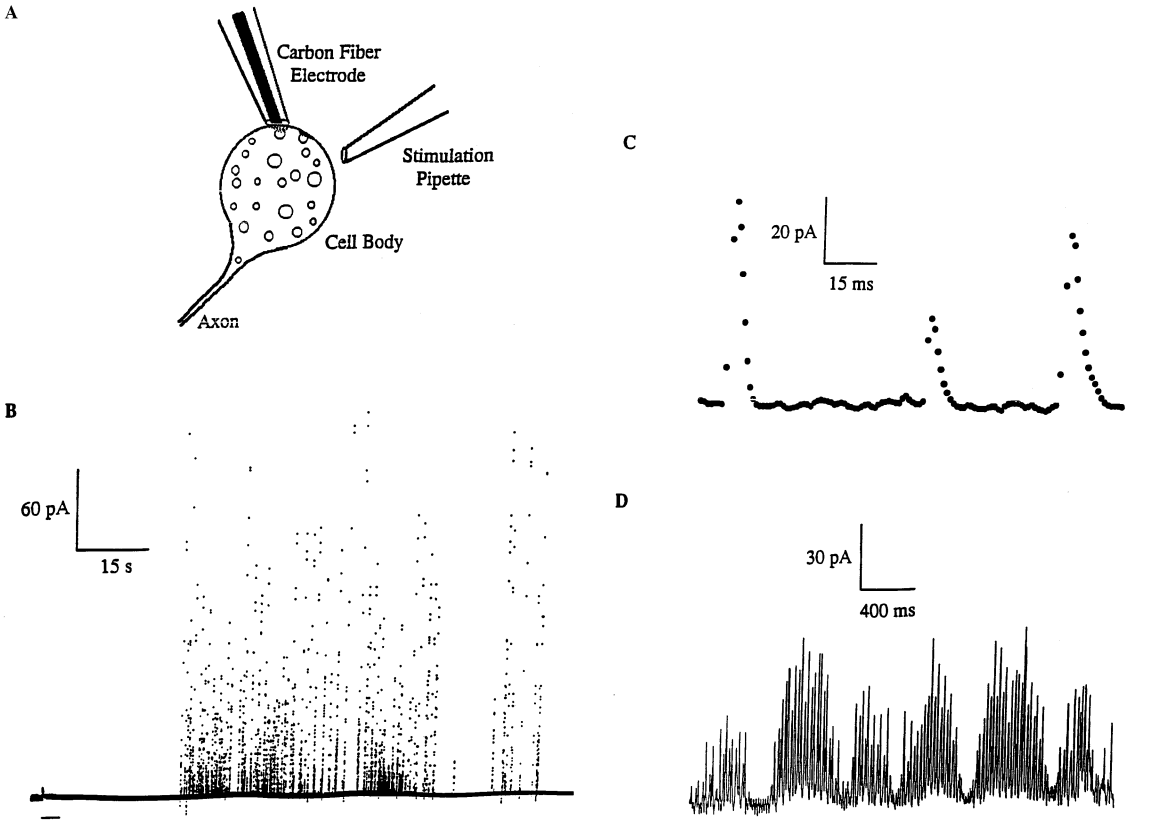

Fig. 6. Dopamine current transients detected by carbon fiber disk electrodes following cellular stimulation: (A) Schematic of a carbon fiber placed on the top of the cell body of an in vivo *Planorbis* dopamine neuron and a stimulation pipette placed close to the cell body; (B) An example of current transients recorded with the amperometric constant-voltage method. A large *Planorbis* dopamine cell (diameter ~ 100 μm) was stimulated with a 4 s pulse (87 nl) of potassium chloride (1 M) delivered from a glass pipette that was placed about 15 μm from the cell body. The stimulation is shown by the horizontal bar below the trace; (C) Examples of the expanded secretory events with base widths ranging from 4 to 40 ms and an average width of 14 ms (13 cells and 12 324 transients). Data points were acquired every 1.0 ms and typical rise times were 2–4 ms; (D) Bursting release events were observed in 24 out of 29 cells that showed release transients. The overall success rate for observation of current transients from cells sampled was $\sim 50\%$. From Chen et al. [5], with permission.

currently being tested by culturing the GDC, whereby removing it from the animal, all synaptic connections will be lost. Another possible explanation for the bursting release is that it is controlled by Ca^{2+} oscillations within the GDC, since Ca^{2+} entry is necessary for exocytosis to occur, and intracellular calcium fluctuations have been correlated to burst firing in neurons [73,74]. This hypothesis is currently being tested by controlling Ca^{2+} entry using selective calcium channel blockers.

One very useful aspect of amperometric detection of exocytosis events is that the data are easily quantified. The number of moles of neurotransmitter (N) is given by Faraday's law, $N = Q/nF$ where Q is the charge (area under each current transient), n is the number of electrons transferred (two for DA), and F is the Faraday constant. By calculating N for many release events, a histogram of vesicle amount can be calculated and is shown in Fig. 7(A). The most interesting feature of Fig. 7(A) is the bimodal distribution of vesicle amount. There is a small distribution of vesicles containing a small amount of DA and a broad

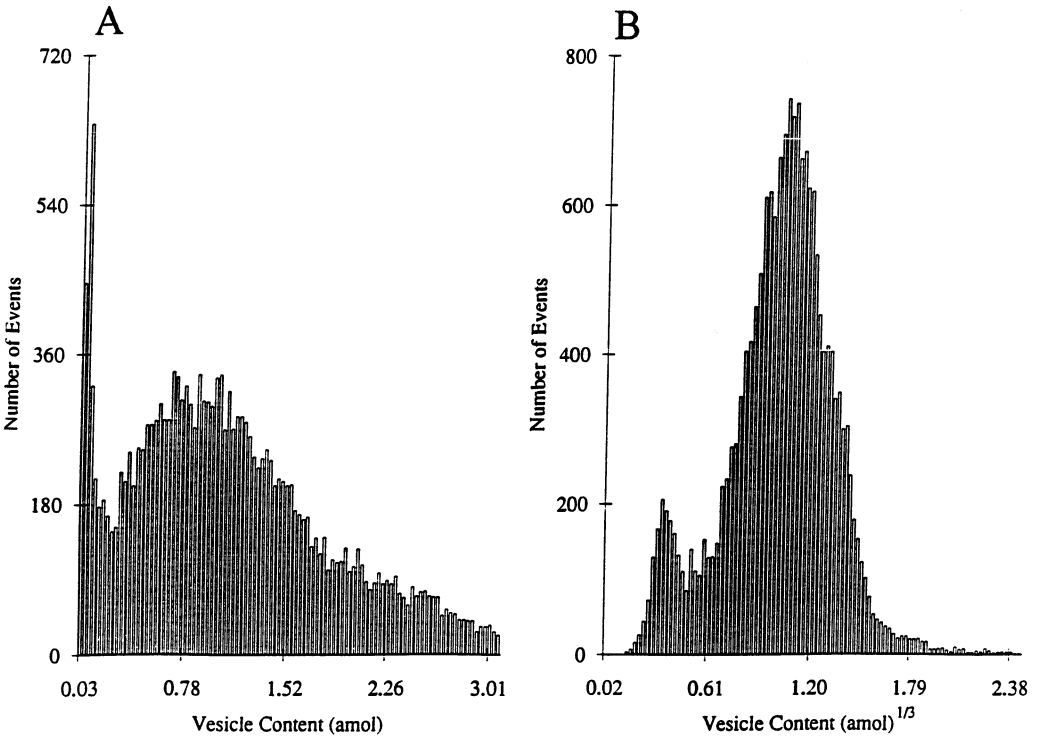

Fig. 7. Histograms of the frequency of release events vs. the amount of neurotransmitter released: (A) Frequency vs. attomoles of dopamine released (16 cells, 18 456 events). Only release events with base widths less than 40 ms were considered. Based on the results obtained from 16 cells, the average vesicle content was 1.36 ± 0.53 amol (mean $\pm$ SD), equivalent to $818\,000 \pm 319\,000$ molecules of dopamine; (B) Frequency vs. the cube root of attomoles of dopamine released (16 cells, 18 456 events). From Chen et al. [5], with permission.

distribution of vesicles with a larger amount of DA. Interestingly, a similar histogram of vesicle amount is seen in the serotonin containing leech neuron [75] and electron microscopy has shown that vesicle size distributions in the leech neuron are characterized by a narrow distribution of small vesicles and a wide distribution of large vesicles [76]. The similarity of the sized distributions from electron microscopy and the vesicle amount distributions from electrochemistry suggest the possibility that the bimodal distribution of vesicle amount is due to different distributions of vesicle size.

Additional indirect evidence that the bimodal distribution results from two distributions of vesicle size is provided by a cube root of vesicle amount histogram as shown in Fig. 7(B). If vesicular DA is present at a uniform concentration, and the vesicular volume is defined by a sphere, then the size of the vesicles should be proportional to the cube root of the amount. The histogram in Fig. 7(B) indeed shows two distributions that appear to be Gaussian, which is consistent with a Gaussian distribution of vesicle radius as observed for other cells in culture [77]. This analysis has been used for other cell lines and the standard deviation of the cube root distribution matches closely the standard deviation a Gaussian distribution of vesicle diameter. The early electron microscopy studies of *P. corneus* vesicle size did not have sufficient resolution to distinguish multiple size distributions [78]. Therefore, electron microscopy studies of vesicle size in the GDC are currently under investigation to determine if the cube root hypothesis is correct for *P. corneus* also.

The data presented here are significant to neuroscience in a number of ways. Microelectochemistry is the only technique currently available that can measure exocytotic release of neurotransmitter on the millisecond time scale. Although this had been demonstrated in vitro, these studies are the first obtained from a single intact neuron still in the animal. Also, the GDC provides a model of neurotransmitter release, by exocytosis, from the cell body of a neuron, thus suggesting a more direct role of the cell body in neurocommunication for certain neurons. In addition to exocytosis, DA release from the GDC soma by reverse transport has been documented.

3.2. Electrochemical measurement of reverse transport from the GDC

Intracellular voltammetry experiments have revealed that influx of DA into the GDC occurs via a DA transporter [8]. This transporter also works in reverse and has been used to investigate the mechanism of action of amphetamine in increasing extracellular DA [6].

There are two hypotheses for the cellular mechanism of amphetamine action. One hypothesis is that amphetamine acts directly on the transporter by competitive inhibition [79]. The other model proposes that amphetamine acts as a weak base to redistribute DA from vesicles to the cytoplasm by collapsing the pH gradient that drives vesicular DA accumulation [6,80,81]. Sulzer et al. [6] have used electrochemistry to provide evidence that the weak base model of amphetamine action is, at least in part, responsible for DA release by reverse transport from the GDC soma.

To show that release occurs by reverse transport, a carbon ring electrode [82] has been micromanipulated to the surface of the cell in a way similar to that shown in Fig. 6(A). Detection is performed by voltammetry. A pulled glass capillary containing 0.5 mM DA is inserted into the cell and 4 pl is injected by pressure into the cytoplasm. Fig. 8(A) shows the resultant rapid increase in extracellular DA to a maximum concentration of 22.5 ± 0.9 μM in 3.5 s. When the physiological saline is replaced with nomifensine (a specific blocker of the DA uptake transporter), the extracellular increase in DA following similar intracellular DA injections is attenuated by $87 \pm 4\%$. The increase in extracellular DA concentration increases to near control levels after removal of the nomifensine solution. Fig. 8(B) shows voltammograms taken following the first, second, and fourth intracellular DA injections and strongly suggests that the released substance is DA.

To test the intracellular action of amphetamine, 8 pl of 100 mM amphetamine has been injected into the cell and the external solution has been monitored voltammetrically. Fig. 8(C) shows the response at an electrode held at a constant potential of 0.8 V. There is a rapid increase in extracellular DA following intracellular injection of amphetamine to a maximum of 1.43 ± 0.58 μM (mean ± SEM). Fig. 8(D) shows that the voltammetry of the released substance matches that for an in vitro DA standard.

Since amphetamine is introduced intracellularly in these experimetns, its action is a result of an intracellular mechanism, not one affecting the DA transporter itself. These data suggest that DA is probably released into the cytosol by the weak base action of amphetamine on the vesicles. The higher cytosolic DA concentration subsequently forces the transporter to work in reverse causing an increase in extracellular DA. Since reverse transport experiments suggest that amphetamine redistributes DA from vesicles into the cytoplasm and actually decreases the quantal size of PC12 cell vesicles [6], and exocytosis experiments show the occurrence of multiple classes of vesicles in the GDC, one is led to question whether amphetamine has a preferential effect on one class of vesicles.

3.3. Dose dependent effect of amphetamine on two classes of vesicles in the GDC

Recent advances in ultrastructural analysis have shown different types of vesicles are sometimes co-localized in neurons [83–89]. They are often referred to as small synaptic vesicles (SSV) and large dense core vesicles (LDCV). It is generally thought the SSV is ready for release and the LDCV acts as a storage container. However, a

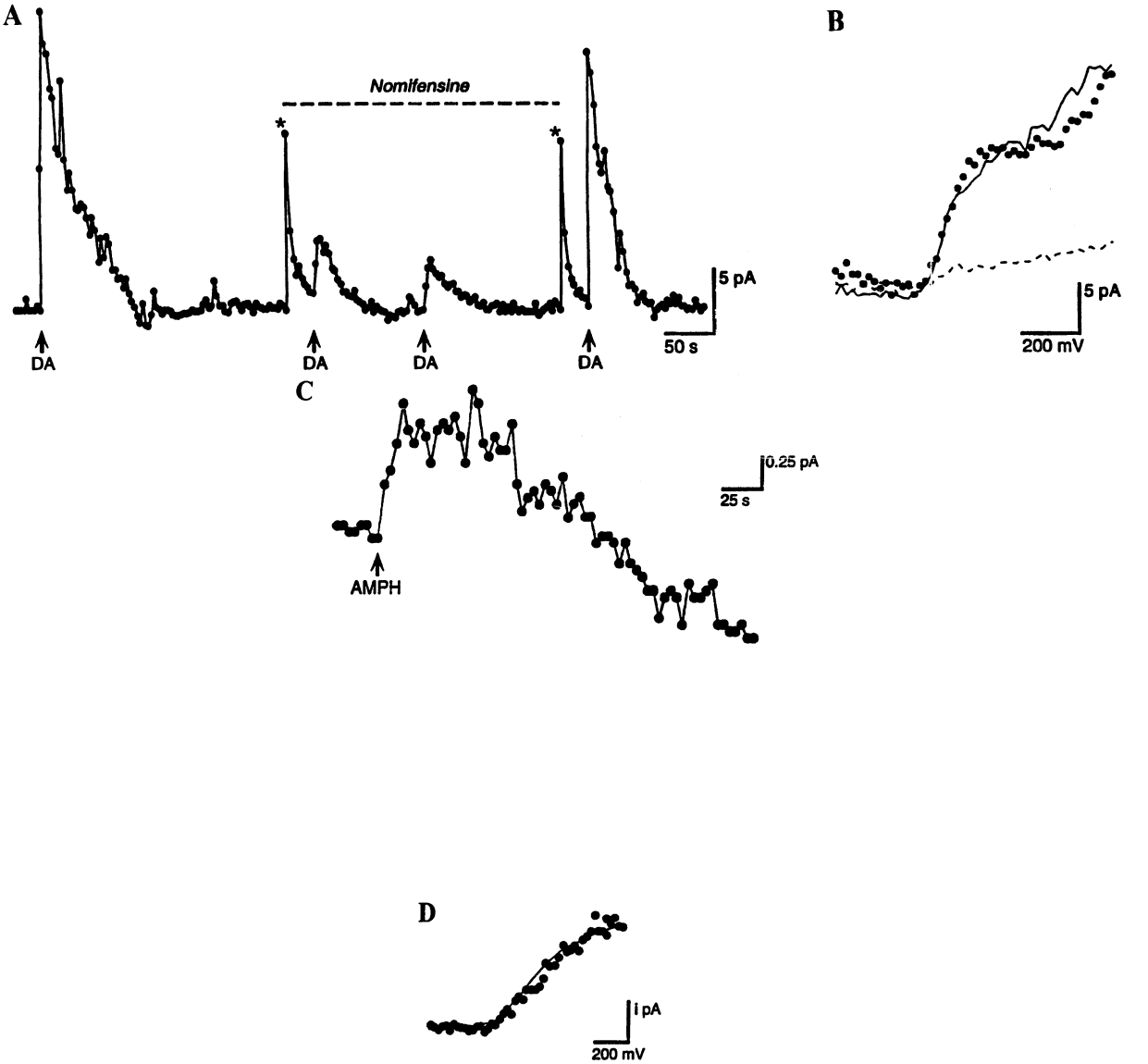

Fig. 8. Intracellular injection of dopamine or amphetamine induces reverse transport: (A) Intracellular injection of 4 pl of 0.5 mM DA (arrows) reliably increases extracellular DA. During extracellular perfusion with 10 μM nomifensine (dashed line), the DA release due to the same DA injections was markedly attenuated. Perfusion with nomifensine-containing medium and its replacement by control medium produce current spikes (asterisks). These data have been baseline corrected by subtracting a curve fitted to the background signal; (B) Background subtracted voltammograms (from -0.2 to 0.8 V) for the first (solid circles), second (dashed line), and fourth (solid line) intracellular DA injections shown in A; (C) Amphetamine (8 pl of 100 mM) was injected intracellularly (arrow), thereby bypassing the uptake transporter, and the increase in extracellular DA measured. Similar levels of DA release were found in three replications of the experiment using DC amperometry; (D) The shape of the voltammogram (-0.2 initial potential to 0.8 V final potential) taken at the peak current value 14 s postinjection (filled circles) closely matched the voltammogram for a DA standard (solid line). Calibration: $I = 0.5$ for the experiment and 31.5 for the standard. From Sulzer et al. [6], with permission.

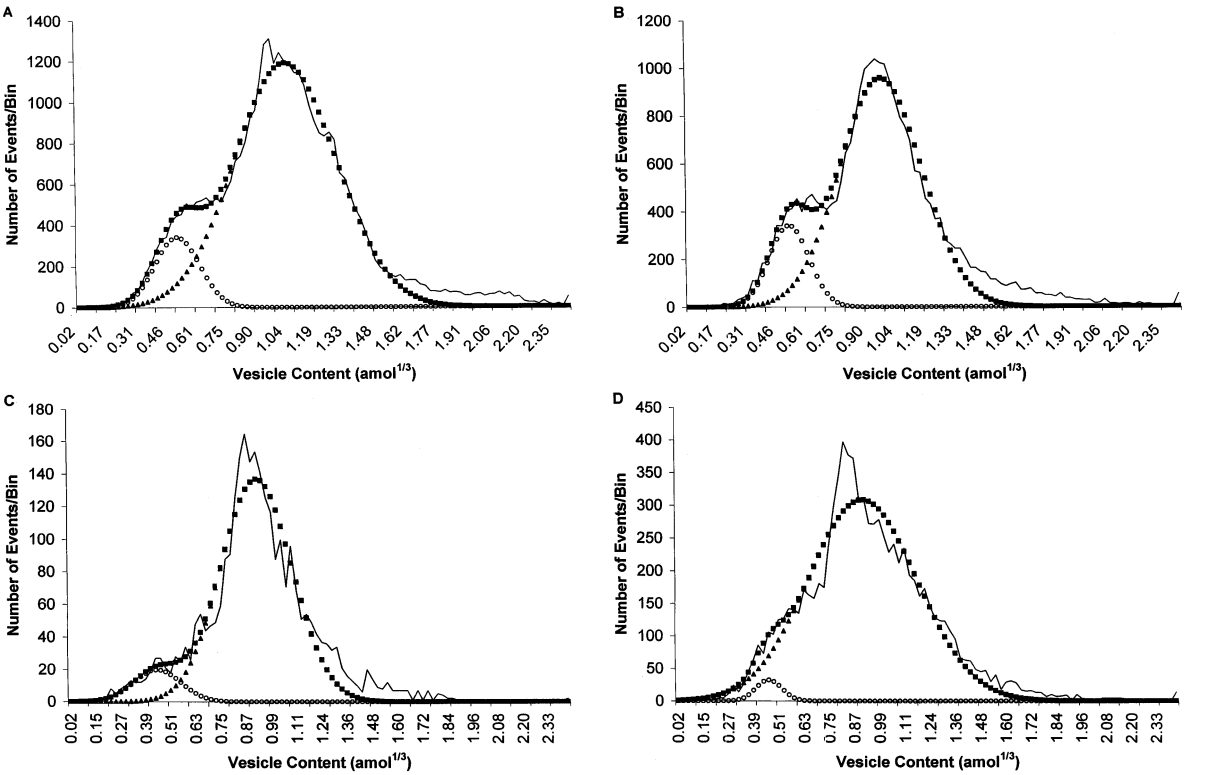

Fig. 9. The effect of amphetamine on two classes of vesicles in the GDC. Histograms (100 bins 0.024 amol/bin) are of the frequency of release events vs. the cube root of attomoles of dopamine released per vesicle. The original data is represented by the solid line. The small Gaussian (open circles), the large Gaussian (closed diamonds) and the sum of the large and small Gaussian (closed boxes), as calculated by equation 1, are also presented in each histogram; (A) Control data (no amphetamine incubation) showing a histogram representing data from 36 304 detected transients from 11 cells; (B) Histogram representing data obtained from seven cells (25 438 transients) after treatment with 10 μM amphetamine; (C) Histogram representing data obtained from four cells (2878 transients) after treatment with 50 μM amphetamine; (D) Histogram representing data obtained from five cells (8875 transients) after treatment with 100 μM amphetamine. From Anderson et al. [7], with permission.

more detailed understanding of the occurrence of co-localized vesicle types is necessary. Since the GDC has been shown to contain multiple vesicle types based on vesicle amount [5], and intracellular amphetamine redistributes vesicular DA to the cytosol [6], it presents an ideal single cell model to determine the effect of amphetamine on multiple classes of vesicles during exocytosis [7,58].

A summary of the effect of amphetamine on two classes of vesicles is shown in Fig. 9. The histograms outlined in Fig. 9 have an abscissa of cube root of vesicle amount. The rationale for the cube root abscissa is discussed above. The solid line represents the original data (normally the bars in a histogram), and the closed boxes are a fit of the entire data set to a double Gaussian function. The open circles and closed diamonds are deconvoluted Gaussians for the small and large distributions, respectively. For simplicity, this manuscript will refer to the small distribution as the small vesicles and the large distribution as large vesicles. Although it might also be possible to explain the bimodal distribution in terms of differential packaging of DA in similarly sized vesicles, the terminology large and small vesicles will be used here.

Fig. 9(A) shows the histogram of the control data (no amphetamine). The number of events in the small Gaussian is 11% of the total number of events and agrees with previous findings [58].

Table 2
Comparison of the dopamine content of vesicles at the peak of each distribution following incubation with amphetamine[a]

Amphetamine concentration (μM)	Dopamine content in the large distribution (amol)	Dopamine content in the small distribution (amol)
Control	1.13	0.13
10	0.91	0.13
50	0.78	0.083
100	0.78	0.097

[a] From Anderson et al. [7], with permission.

When treated with 10 μM amphetamine, the number of small vesicles released from the GDC increases to 14% of the total number of release events, which is slightly greater than that of control. For 50 and 100 μM amphetamine treatment the number of small events decreases to 8.8 and 2.4% of the total number of events (Fig. 9(C, D). These data indicate that amphetamine at a low dose primarily acts on the larger class of vesicles while the small ones are resistant. It is possible that the larger vesicles are depleted in a way that they become small vesicles. Then, at high amphetamine concentration, the small vesicles are virtually eliminated.

Even though it is not statistically different, there is an apparent amphetamine dose dependent shift in the midpoints of the Gaussians. Table 2 shows that, for low amphetamine concentration, the midpoint of the small Gaussian is unchanged. However, for 50 and 100 μM amphetamine, the midpoint of the small distribution differs by at least 25% from the control and 10 μM experiments. For the large Gaussian, there is an apparent dose dependent decrease in the amount of DA as the amphetamine concentration is increased. In agreement with other data, the mean content for all release events for all concentrations of amphetamine studied is significantly different from control.

One explanation for this action of amphetamine on vesicles is that at low concentration it binds with the vesicular DA transporter. At higher amphetamine concentration, the apparent dose dependent depletion is likely due to alkalization by the weak base model discussed above. These are exciting data as they are the first evidence for a differential effect of a psychostimulant on two classes of vesicles and could provide a mechanism to explain the dose dependent effect of different psychostimulants on behavior.

4. Conclusions

It is obvious that electrochemistry, when used alone or in conjunction with a microcolumn separation technique, is extremely useful for single cell analysis. The GDC provides an excellent single cell model of neurotransmission for study by electrochemical methodology. Many questions and concepts important to neuroscience have been strengthened or challenged by studying DA dynamics in and at the GDC. Exocytotic release of DA from the cell body from multiple classes of vesicles that have a differential sensitivity to amphetamine is important for several reasons. It is an example of neurotransmission at a site other than the synapse. It opens up the question of the function of multiple classes of vesicles. It is possible that the differential effect of amphetamine on multiple classes of vesicles could provide an explanation for psychostimulant concentration dependent behavior.

Reverse transport experiments allow the intracellular mechanism of action of amphetamine to be studied. These experiments provide strong evidence that amphetamine primarily acts as a weak base to redistribute DA from vesicles resulting in transport of DA out of the cell, thereby increasing the extracellular DA concentration. Another important aspect of the reverse transport experiment is that it gives a likely explanation for how a psychostimulant like amphetamine modifies behavior by increasing extracellular DA.

CE-EC allows the investigation of several static chemical properties of the GDC. DA appears to be stored in two distinct compartments in the GDC and this appears to be consistent with earlier experiments suggesting functional and reserve compartments in whole animal studies. The cytoplasmic DA concentration as measured by CE-EC is in agreement with the value estimated by in vivo voltammetry. Additionally, primary amines have been profiled in single GDCs with CE-EC and primary amine derivatization with NDA. Without the NDA derivatization, amines such as amino acids are not readily detected by electrochemistry. Thus, CE-EC is a powerful tool to examine the chemistry of single nerve cells. Together, microelectrochemistry and CE-EC at the GDC have provided new insights, as well as new questions, about the chemistry and function of nerve cells.

Acknowledgements

Support from the National Science Foundation and the National Institutes of Health is gratefully acknowledged. We would also like to thank all our coworkers for the work referenced herein.

References

[1] G. Chen, A.G. Ewing, Crit. Rev. Neurobiol. 11 (1997) 59–90.
[2] R.A. Clark, A.G. Ewing, Mol. Neurobiol. 15 (1997) 1–16.
[3] F.D. Swanek, B.B. Anderson, A.G. Ewing, J. Microcol. Sep. (in press).
[4] H.K. Kristensen, Y.Y. Lau, A.G. Ewing, J. Neurosci. Methods 51 (1994) 183–188.
[5] G. Chen, P. F. Gavin, G. Luo, A. G. Ewing, J. Neurosci. 15 (1995) 7747–7755.
[6] D. Sulzer, T.K. Chen, Y.Y. Lau, H. Kristensen, S. Rayprot, A.G. Ewing, J. Neurosci. 15 (1995) 4102–4108.
[7] B.B. Anderson, G.Chen, D.A. Gutman, A.G. Ewing, Brain Res. (in press).
[8] J.B. Chien, R.A. Wallingford, A.G. Ewing, J. Neurochem. 54 (1990) 633–638.
[9] N.N. Osborne, E. Priggemeier, V. Neuhoff, Brain Res. 90 (1975) 261–271.
[10] B.B. Anderson, A.G. Ewing, D. Sulzer, Methods Enzymol. (in press).
[11] R.N. Adams, Anal. Chem. 48 (1976) 1128–1138.
[12] R.M. Wightman, Anal. Chem. 53 (1981) 1125–1134.
[13] R.M. Wightman, Science 240 (1988) 415–420.
[14] A. Meulemans, B. Poulain, G. Baux, L. Tauc, D. Henzel, Anal. Chem. 58 (1986) 2088–2092.
[15] Y.Y. Lau, J.B. Chien, D.K.Y. Wong, A.G. Ewing, Electroanalysis 3 (1991) 87–95.
[16] D.J. Leszczyszyn, J.A. Jankowski, O.H. Viveros, E.J. Diliberto Jr., J.A. Near, R.M. Wightman, J. Biol. Chem. 265 (1990) 14736–14737.
[17] A.G. Ewing, T.K. Chen, in: Adams, R. (Ed.), Neuromethods: In Vivo monitoring, Humana Press, Clifton, NJ, 1995, pp. 269–304.
[18] E.W. Kristensen, W.G. Kuhr, R.M. Wightman, Anal. Chem. 59 (1987) 1752–1757.
[19] T.K. Chen, G. Luo, A.G. Ewing, Anal. Chem. 66 (1994) 3031–3035.
[20] J.E. Baur, E.W. Kristensin, L.J. May, D.J. Wiedemann, R.M. Wightman, Anal. Chem. 60 (1988) 1268–1272.
[21] J.M. Mesaros, A.G. Ewing, P.F. Gavin, Anal. Chem. 66 (1994) 527A–537.
[22] J. Bergquist, A. Tarkowski, R. Ekman, A.G. Ewing, Proceedings of the National Academy of Science USA, vol. 91, 1994, pp. 12912–12916.
[23] B.L. Hogan, E.S. Yeung, Anal. Chem. 64 (1992) 2841.
[24] T.T. Lee, E.S. Yeung, Anal. Chem. 64 (1992) 1226–1231.
[25] Q. Xue, E.S. Yeung, J. Chromatogr. A 661 (1994) 287–295.
[26] Q. Xue, E.S. Yeung, Anal. Chem. 66 (1994) 3575–3580.
[27] S.A. Shippy, J.A. Jankowski, J.V. Sweedler, Anal. Chim. Acta 307 (1995) 163–171.
[28] S.A. Hofstadler, J.C. Severs, R.D. Smith, F.D. Swanek, A.G. Ewing, Rapid Commun. Mass Spectrom. 10 (1996) 919–922.
[29] Z. Rosenzweig, E.S. Yeung, Anal. Chem. 66 (1994) 1771.
[30] R.A. Wallingford, A.G. Ewing, Anal. Chem. 60 (1988) 1972–1975.
[31] T.M. Olefirowicz, A.G. Ewing, Anal. Chem. 62 (1990) 1872–1876.
[32] T.M. Olefirowicz, A.G. Ewing, J. Neurosci. Methods 34 (1990) 11–15.
[33] T.M. Olefirowicz, A.G. Ewing, Chimia 45 (1991) 106–108.
[34] S. Sloss, A.G. Ewing, Anal. Chem. 65 (1993) 577–581.
[35] S.S. Ferris, G. Lou, A.G. Ewing, J. Microcol. Sep. 6 (1994) 263–268.
[36] B. Powell, G.A. Cottrell, J. Neurochem. 22 (1974) 605–606.
[37] C. Marsden, G.A. Kerkut, Comput. Gen. Pharmacol. 1 (1970) 101–116.
[38] M. J. Besson, A. Cheramy, P. Feltz, J. Glowinski, Proc. Natl. Acad. Sci. USA 62 (1969) 741–748.
[39] A.G. Ewing, J.C. Bigelow, R.M. Wightman, Science 221 (1983) 169–171.
[40] J.G. White, R.L. St. Claire, J.W. Jorgenson, Anal. Chem. 58 (1986) 293.

[41] R.T. Kennedy, R.L. St. Claire, J.G. White, J.W. Jorgenson, Mikrochim. Acta 11 (1987) 37–45.
[42] R.T. Kennedy, J.W. Jorgenson, Anal. Chem. 61 (1989) 436–441.
[43] A. Trojanek, H. De Jong, Anal. Chim. Acta 11 (1992) 325.
[44] F.D. Swanek, G. Chen, A.G. Ewing, Anal. Chem. 68 (1996) 3912–3916.
[45] M.C. Roach, M.D. Harmony, Anal. Chem. 59 (1987) 411.
[46] F. de Montigny, J.F. Stobaugh, R.S. Givens, R.G. Carlson, K. Srinivasachar, L.A. Sternson, T. Higuchi, Anal. Chem. 59 (1987) 1096.
[47] B.K. Matuszewshi, R.S. Givens, K. Srinivasachar, R.G. Carlson, T. Higuchi, Anal. Chem. 59 (1987) 1102.
[48] R.T. Kennedy, M.D. Oates, B.R. Cooper, B. Nickerson, J.W. Jorgenson, Science 246 (1989) 57–63.
[49] A.M Hoyt Jr., S.C. Beale, J.P. Larmann Jr., J.W. Jorgenson, J. Microcol. Sep. 5 (1993) 325–330.
[50] M.D. Oates, J.W. Jorgenson, Anal. Chem. 61 (1989) 432–435.
[51] M.D. Oates, B.R. Cooper, J.W. Jorgenson, Anal. Chem. 62 (1990) 1573–1577.
[52] S.D. Gilman, A.G. Ewing, Anal. Chem. 67 (1995) 58–64.
[53] S.D. Gilman, A.G. Ewing, Anal. Methods Instrum. 2 (1995) 133–141.
[54] T.J. O'Shea, M.W. Telting-Diaz, S.M. Lunte, C.E. Lunte, M.R. Smyth, Electroanalysis 4 (1992) 463–468.
[55] T.J. O'Shea, R.D. Greenhagen, S.M. Lunte, C.E. Lunte, M.R. Smyth, N. Wanatabe, J. Chromatogr. 593 (1992) 305–312.
[56] R.S. Kelly, R.M. Wightman, Anal. Chim. Acta 187 (1986) 79–87.
[57] R.A. Clark, A.G. Ewing, Mol. Neurobiol. 15 (1997) 1–16.
[58] G. Chen, A.G. Ewing, Brain Res. 701 (1995) 167–174.
[59] P. Garris, R.M. Wightman, J. Neurosci. 14 (1994) 6084.
[60] M.J. Heeringa, E.D. Abercrombie, J. Neurochem. 65 (1995) 192–200.
[61] A. Cheramy, V. Leviel, J. Glowinski, Nature 289 (1981) 537–542.
[62] C. Gauchy, M. L. Kernel, M. Desban, R. Romo, J. Glowinski, M.J. Besson, Neurosci. 22 (1987) 935–956.
[63] M.A. Klitenick, P. DeWitte, P.W. Kalivas, J. Neurosci. 12 (1992) 2623–2632.
[64] D. A. Johnson, G. Pilar, J. Physiol. (Lond.) 299 (1980) 605–619.
[65] K. Suetake, H. Kojima, K. Inanaga, K. Kotetsu, Brain Res. 205 (1981) 436–440.
[66] D.V. Pow, J.F. Morris, Neuroscience 32 (1989) 435–439.
[67] W. Lichtensteiger, D. Felix, F. Hefti, Brain Res. 170 (1979) 241–254.
[68] Y. Archavsky, T.G. Deliagina, G.N. Orlovsky, Y. Panchin, Exp. Brain Res. 70 (1988) 323–331.
[69] E.A. Marcus, T.J. Carew, J. Neurobiol. 22 (1991) 418–429.
[70] B. Jagadeesh, C.M. Gary, D. Ferster, Science 222 (1992) 552–554.
[71] M. Kukuljan, S.S. Stojilkovi, E. Rojas, K.J. Catt, FEBS Lett. 301 (1992) 19–22.
[72] D.L. Cardozo, Neuroscience 56 (1993) 409–421.
[73] C. Randriamampita, R.Y. Tsien, Nature 364 (1993) 809–814.
[74] A. Tse, F.W. Tse, W. Almers, B. Hille, Science 260 (1993) 82–84.
[75] D. Bruns, R. Jahn, Nature 377 (1995) 62–65.
[76] L.P. Henderson, D.P. Kuffler, J.G. Nicholls, R.J. Zhang, J. Physiol. 340 (1983) 347–358.
[77] J.M. Finnegan, K. Pihel, P. Cahill, L. Huang, S. E. Zerby, A.G. Ewing, R.T. Kennedy, R.M. Wightman, J. Neurochem. 66 (1996) 1914–1923.
[78] V.W. Penreath, M.S. Berry, J. Neurocytol. 4 (1975) 249–260.
[79] J.F. Fischer, A.K. Cho, J. Pharmacol. Exp. Ther. 208 (1979) 203–209.
[80] D. Sulzer, S. Rayport, Neuron 5 (1990) 797–808.
[81] D. Sulzer, N.T. Maidment, S.J. Rayport, J. Neurochem. 60 (1993) 527–535.
[82] Y.T. Kim, D.M. Scarnulis, A.G. Ewing, Anal. Chem. 58 (1986) 1782–1786.
[83] G.D. Fox, D. Kötting, G.H.C. Dowe, Brain Res. 498 (1989) 279–288.
[84] M.L. Kiene, H. Stadler, EMBO J. 6 (1987) 2209–2215.
[85] S. Masuko, T. Chiba, Cell Tissue Res. 253 (1988) 507–516.
[86] A.J. Smolen, J. Electron Microsc. Tech. 10 (1988) 187–204.
[87] J.J. Soghomonian, L. Descarries, J. Lanoir, Neuroscience 17 (1986) 1147–1157.
[88] H. Stadler, M.L. Kiene, EMBO J. 6 (1987) 2217–2221.
[89] L.S. Swales, I. Cournil, P.D. Evans, Tissue Cell 24 (1992) 547–558.
[90] F.D. Swanek, Ph.D. Thesis, Chapter 1, 1996.